Practically Feasible Histogram-Mode and List-Mode EM Reconstructions with Full Motion Compensation

Arman Rahmim, Peter Bloomfield, Sylvain Houle, Mark Lenox, Christian Michel, and Vesna Sossi

Abstract— **With continuous improvements in spatial resolution of PET scanners, small patient movements during PET imaging become a significant source of resolution degradation. This work explores incorporation of motion information into EM reconstruction algorithms. Pre-correction of the data for attenuation and normalization as well as weighted schemes, in which these correction factors are incorporated into the system matrix, are considered. An important issue addressed is the existence of LORs corresponding to no actual pairs of detectors and their motion-induced "interaction" with the detectable LORs. An example of this is a scanner design with gaps existing in-between the detector heads. It is shown that to properly account for such LORs in histogram-mode and list-mode EM reconstructions, in addition to motion-correction of the data, the algorithms themselves must be modified. This modification is implemented by including time-weighted sensitivity correction factors. A practically feasible method for calculation of sensitivity factors is derived based on image-space monitoring of voxel motion during the scan.**

I. Introduction

Recent developments in 3D positron emission tomography (PET) systems have enabled the spatial resolution to reach the 2-3mm FWHM range. With such improvements in spatial resolution, small patient movements during PET imaging become a significant source of resolution degradation. One method to correct for patient movement involves gating of detected events into multiple acquisition frames (MAF), with the use of an external monitoring system, followed by spatial registration and then summation of reconstructions from the acquired frames [1], [2]. However, in the MAF approach, the presence of considerable movement can result in many low-count frames, and furthermore, frames with the object partially exiting the FOV can not be considered (due to an introduced bias in the final sum).

Compensation of individual lines-of-response (LORs) for motion has alternatively been suggested to achieve optimal reconstruction [3]. To this end, motion tracking systems have been used for accurate real-time measurements of position and orientation of the patient (see, for instance, Ref. [4] for *Polaris*, a system based on opto-electronic position sensitive detectors), which in the histogram-mode approach, introduces an event-by-event rebinning technique, resulting in motion-compensated sinograms. These sinograms are subsequently reconstructed using any of the common reconstruction algorithms [5].

However, it can be argued that reconstructing from motion-corrected sinograms or directly from list-mode data can produce image artifacts if motion correction is performed on a purely event-driven (as compared to a more comprehensive modeling of the image-data relation). This is because one can observe [6] that certain events that would have been detected in some LORs may have exited the PET scanner (e.g. axially or through detector gaps) undetected due to object motion. Regular reconstruction methods do not employ knowledge of missing data, and therefore would assume simply that nothing was detected.

We further note that the converse also requires consideration: upon transformation of certain LORs along which the events are detected to LORs along which the events would have been detected, had the object not moved, the calculated LORs may correspond to no actual detector pairs. In other words, motion can result in some LORs which correspond to undetectable regions to exhibit non-zero probabilities of detection, which also needs to be properly modeled. Taking these effects into consideration, it is therefore *not* sufficient to merely motion-correct the events, rather one must also modify the algorithms themselves. Sections II and III discuss incorporation of an exact modeling of motion into the histogram-mode and list-mode EM reconstruction.

II. Motion Correction in Histogram-mode EM Reconstruction

Denoting λ_j^m as the image intensity in voxel j (j=1...J) at the m^{th} iteration, and p_{ij} as the probability of an emission from voxel j being detected along LOR i, the histogram-mode EM algorithm is given by

$$\lambda_j^{m+1} = \frac{\lambda_j^m}{\sum_{i=1}^{I} p_{ij}} \sum_{i=1}^{I} p_{ij} \frac{n_i}{\sum_{b=1}^{J} p_{ib} \lambda_b^m} \qquad (1)$$

where n_i refers to the number of events detected along LOR i (i=1...I). The sensitivity correction factor s_j=$\sum_{i=1}^{I} p_{ij}$ is a summation over all possible measurable LORs (i=1...I) and calculates the probability of an emission from voxel j being detected anywhere (constructive summation is performed over those LORs for which $p_{ij} \neq 0$).

In the original EM algorithms, the data were corrected for attenuation and normalization prior to reconstruction. However,

Manuscript received October 29, 2003.

A. Rahmim and V. Sossi are with Department of Physics and Astronomy, University of British Columbia, Vancouver, BC Canada (e-mail rahmim@physics.ubc.ca, vesna@physics.ubc.ca).

P. Bloomfield and S. Houle are with Vivian M Rakoff PET Centre, Centre for Addiction and Mental Health, Toronto, ON Canada (email peter.bloomfield@camhpet.ca,sylvain.houle@camhpet.ca).

M. Lenox and C. Michel are with CPS Innovations, Knoxville, TN USA (email Mark.Lenox@cpspet.com, Christian.Michel@cpspet.com).

0-7803-8257-9/04/$20.00 © 2004 IEEE.

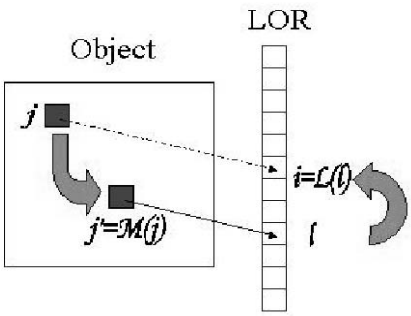

Fig. 1. An event detected at an LOR l generated in voxel j, which has been translated to voxel $j' = \mathcal{M}(j)$ at time of detection, would have been detected at LOR $i = \mathcal{L}(l)$ if the object had not moved.

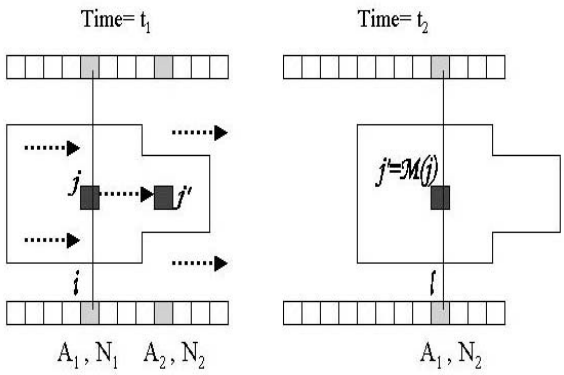

Fig. 2. An event detected at time t_2 along an LOR l, which would have been detected along an LOR i if the object had not moved, has the *same* attenuation correction factor as measured for A_i at time t_1. The normalization correction factor however is LOR-specific and changes with motion.

it was later proposed that these corrections could be included in the algorithm as weighting factors [7]. This can be accomplished by noting that the system matrix P=$(p_{ij})_{I\times J}$ may be more generally written as P=WG where G=$(g_{ij})_{I\times J}$ is the geometric probability of an event generated at voxel j to be detected at LOR i, and the diagonal matrix W=$(w_i)_{I\times I}$ allows a weight to be assigned to each LOR, to account for sensitivity variations. Substituting $p_{ij} = w_i g_{ij}$ into Eq. (1) results in the emergence of cancellation of w_i in the back- and forward-projection steps. , thus giving:

$$\lambda_j^{m+1} = \frac{\lambda_j^m}{\sum_{i=1}^{I} w_i g_{ij}} \sum_{i=1}^{I} g_{ij} \frac{n_i}{\sum_{b=1}^{J} g_{ib}\lambda_b^m} \qquad (2)$$

A. Modification of the Histogram-mode EM Algorithm

Once a motion-corrected sinogram is obtained, some LORs may be transformed into undetectable LORs (i.e. LORs for which no actual pair of detectors exist). On the other hand, some detectable LORs exhibit less counts that they would have, had the object not moved, since corresponding events passed through undetectable LORs. These missing LORs can in principle be located: i) radially out of the field of view. ii) axially out of the scanner, or iii) in regions corresponding to gaps in between the detectors.

The first case may be ignored as it can be safely assumed that the object stays in the radial field of view of the scanner all the time, whereas the second case is especially important in 3D PET imaging in which small rotations in the object can result in many LORs to exit the FOV axially, and vice versa. The third possibility is expected to be significant in non-cylindrical designs. In the octagonal design of the high resolution tomograph (HRRT) [8], for instance, gaps existing between the eight detector heads of the scanner occupy over 10% of the sinogram space.

The system element p_{ij} therefore needs to be modified to take into account the aforementioned issues in calculation of the probability of detection along any LOR i of an event emitted in any voxel j. In this regard, we first introduce an invertible operator $\mathcal{L}$ which transforms the LOR along which an event *is* detected at time t into the corresponding LOR along which the event *would* have been detected had the object not moved. An instance of this is shown in Fig. (1), where an event generated from a voxel j, currently located at a position j' due to some transformation $\mathcal{M}(j)$, has been detected along an LOR l, and therefore must be histogrammed along the motion-corrected LOR i=$\mathcal{L}(l)$, as is shown.

Thus, when correcting for motion with respect to t=0, the geometric probability g_{lj}^t (where the superscript t indicates knowledge of object orientation and position with respect to the origin of the time axis[1]) of an event generated in voxel j being detected in LOR l at a given time t must be equal to the probability of it being detected in LOR i at t=0 where $i = \mathcal{L}_t(l)$; That is

$$g_{lj}^t = g_{ij}^0 \quad \text{where} \quad i = \mathcal{L}_t(l) \qquad (3)$$

or more compactly

$$g_{lj}^t = g_{\mathcal{L}_t(l)j}^0 \qquad (4)$$

Denoting N_i and A_i as the attenuation and detector normalization factors for an LOR i, incorporation of these factors in presence of motion must now be addressed. In the unweighted scheme, these factors are applied onto the acquired LOR events that are histogrammed into appropriate motion-compensated sinogram bins. Alternatively, in weighted schemes, one or both of these factors are instead used inside the reconstruction algorithm itself. The normalization factor for an LOR l along which an event is detected is given by the value of N_l for the LOR itself, independent of any motion. However, this is *not* the case for attenuation correction, in which case the factor is given by the value of the attenuation factor at LOR i along which the event would have been detected had the object not moved. This is depicted in Fig. (4).

[1]It is often assumed that the patient does not move between the attenuation scan and the start of the emission scan. Nevertheless, the more general case of having the patient move between the two scans can be treated by motion-correcting with respect to the time at which the attenuation scan was performed.

It follows that, defining

$$Z_l = \begin{cases} 0 & \text{if} \quad N_l = 0 \\ 1 & \text{if} \quad N_l \neq 0 \end{cases} \tag{5}$$

such that $\{l|Z_l = 0\}$ is the set of all LORs not detectable by the scanner, and

$$l(i,t) \equiv \mathcal{L}_t^{-1}(i) \tag{6}$$

the weighting factor $w_{l(i,t)}$ for any LOR $l(i,t)$ can be written as

$$w_{l(i,t)} = \begin{cases} 1 * Z_{l(i,t)} & \text{Unweighted} \\ N_{l(i,t)} & \text{N-weighted} \\ A_i * Z_{l(i,t)} & \text{A-weighted} \\ A_i N_{l(i,t)} & \text{AN-weighted} \end{cases} \tag{7}$$

Introducing M=$(m_{ij})_{I\times J}$ as the motion-compensated system matrix, m_{ij} must indicate the probability, for the course of the *entire* scan, that an event generated in object voxel j is finally binned into LOR i. It must therefore incorporate time-weighted probability-of-detection ($w_{l(i,t)}g^t_{l(i,t)j}$) contributions from any LOR $l(i,t)$ that could record events that would have been detected in LOR i had the object not moved; i.e.

$$m_{ij} = \frac{1}{T}\int_0^T w_{l(i,t)} g^t_{l(i,t)j} dt \tag{8}$$

which using Eq. (3) can be simplified to

$$m_{ij} = \frac{1}{T} g^0_{ij} \int_0^T w_{l(i,t)} dt \tag{9}$$

In the AN-weighted scheme, for instance, one would have

$$m_{ij} = \frac{1}{T} g^0_{ij} A_i \int_0^T N_{l(i,t)} dt \tag{10}$$

which upon replacing p_{ij} in Eq. (1), and dropping the superscript of g^0_{ij} for convenience, after cancellations, results in the following AN-weighted reconstruction algorithm:

$$\lambda_j^{m+1} = \frac{\lambda_j^m}{\frac{1}{T}\sum_{i=1}^I g_{ij} A_i \int_0^T N_{l(i,t)} dt} \sum_{i=1}^I g_{ij} \frac{n_i}{\sum_{b=1}^J g_{ib}\lambda_b^m} \tag{11}$$

Here, the back-projection summations are performed over all observed counts including, for instance, those that do not correspond to existing detector pairs (whenever $n_i \neq 0$, it is necessarily the case that $m_{ij} \neq 0$ and therefore cancellation of attenuation and normalization components of m_{ij} in the back- and forward-projection steps is valid).

B. A Practical Method for Calculation of Sensitivity Factors

We have shown that the sensitivity correction factor s_j at any voxel j is given by

$$s_j = \frac{1}{T}\sum_{i=1}^I g_{ij} A_i \int_0^T N_{l(i,t)} dt \tag{12}$$

in the AN-weighted scheme. Calculation of s_j therefore requires integrating over entire duration of scan to derive the properly motion-corrected normalization factors, which are subsequently back-projected along with the attenuation factors. This should be performed for *all* LORs, which can include LORs that do not correspond to actual detector pairs. This calculation can therefore be extremely time-consuming for high resolution scanners. One method to address it would be to approximate the object to be static in time intervals within which motion is relatively small in order to simplify calculation of summation over time. Nevertheless, this approach is bound to lead to artifacts for the general case of continuous motion.

To better address this issue, we make the following very useful observation: at any given time t, calculation of the time-dependent geometric factor g^t_{lj} (as shown in Eq. 3) can be performed in another way: instead of mapping LOR l into a motion-corrected LOR i, one can map the object voxel j to the new voxel it has moved to (i.e. $j'(j,t)$≡$\mathcal{M}_t(j)$) at time t, where $\mathcal{M}_t$ is an image-based motion-tracking operator, as depicted in Fig. 1. Mathematically, we have the following identity:

$$g_{ij} \equiv g_{l(j,t)j'(j,t)} \tag{13}$$

The above relation can lead to considerable speed increase in calculation of s_j for schemes in which data are pre-corrected for attenuation (i.e. unweighted and N-weighted schemes), as we show here. In the N-weighted scheme, for instance, we have

$$\lambda_j^{m+1} = \frac{\lambda_j^m}{\overline{s}_j} \sum_{i=1}^I g_{ij} \frac{n_i/A_i}{\sum_{b=1}^J g_{ib}\lambda_b^m} \tag{14}$$

where $\overline{s}_j$ is given by

$$\overline{s}_j = \frac{1}{T}\sum_{i=1}^I g_{ij} \int_0^T N_{l(i,t)} dt = \frac{1}{T}\int_0^T \sum_{i=1}^I g_{ij} N_{l(i,t)} dt \tag{15}$$

We next note that the summation over *all* i in the above equation involves consideration of all l=$l(i,t)$, and thus the summation index i can as easily be replaced by l. Combining this observation with Eq. (13) gives

$$\overline{s}_j = \frac{1}{T}\int_0^T \sum_l g_{lj'(j,t)} N_l \tag{16}$$

and therefore

$$\overline{s}_j = \frac{1}{T}\int_0^T s_{j'(j,t)} dt \quad \text{where} \quad s_j = \sum_l g_{lj} N_l \tag{17}$$

In other words, in the calculation of $\overline{s}_j$ for any voxel j, instead of having to perform time-averaging in the LOR domain, one can do so in the image domain, by evaluating sensitivity factors (which are calculated once for the object at t=0) at voxels $j'(j,t)$ over time. This corresponds to monitoring the motion of voxel j with time. Since with current, high-resolution scanners, the LOR domain is typically much larger than the image domain, the proposed method would allow a considerable speed-up in correct reconstruction of motion-corrected sinograms. As we shall show, this technique will also be applicable to list-mode reconstruction.

III. Motion Correction in List-mode EM Reconstruction

One must observe that while motion-compensated histogramming involves interpolating the transformation $\mathcal{L}_t(l)$ into an actual sinogram bin i, in the case of list-mode reconstruction one can work with LOR coordinates, as compared to rebinned LOR positions, thus potentially improving resolution. In this regard, g^t_{lj}, the geometric probability at time t of detecting an event generated at voxel j along an LOR l, can be expressed as $g_j(\mathbf{i}(\mathbf{l},\mathbf{t}))$, where $\mathbf{i}(\mathbf{l},\mathbf{t})$, a continuous variable, holds the exact coordinates of LOR l after being motion-corrected.

The list-mode expectation maximization (LM-EM) reconstruction algorithm has been previously formulated by Parra and Barrett [9]. Following the same approach, we have shown that consideration of motion results in the following EM algorithm:

$$\lambda_j^{m+1} = \frac{\lambda_j^m}{\int_0^T s_j^t dt} \sum_{k=1}^{N} g_j(\mathbf{i}(\mathbf{l_k},\mathbf{t})) \frac{1}{\sum_{b=1}^{J} g_b(\mathbf{i}(\mathbf{l_k},\mathbf{t}))\lambda_b^m} \quad (18)$$

where l_k is the LOR along which the kth event is detected (k=1...N) and s_j^t is a time-dependent sensitivity correction factor: the probability at time t that an emission from voxel j is detected anywhere. The overall time-averaged sensitivity correction factor $\overline{s}_j \equiv \int_0^T s_j^t dt$ can be calculated on an LOR-domain approach such that any LOR l is transformed to the corresponding motion-corrected LOR i=$i(l,t)$ for the calculation of time-dependent attenuation and geometric factors; i.e.:

$$\overline{s}_j = \frac{1}{T}\int_0^T s_j^t = \frac{1}{T}\int_0^T \sum_l g_{i(l,t)j} A_{i(l,t)} N_l dt \quad (19)$$

which has also been suggested by Qi and Huesman [10] in an effort to maximize the log-likelihood function of list-mode data.

Nevertheless, similar to approach of Sec. II-B, we notice that in the N-weighted scheme (with results again directly applicable to the unweighted scheme), again using Eq. (13), one can write

$$\overline{s}_j = \frac{1}{T}\int_0^T \sum_l g_{i(l,t)j} N_l = \frac{1}{T}\int_0^T \sum_l g_{lj'(j,t)} N_l \quad (20)$$

which reproduces Eq. (16). Therefore, we propose the following N-weighted algorithm:

$$\lambda_j^{m+1} = \frac{\lambda_j^m}{\overline{s}_j} \sum_{k=1}^{N} g_j(\mathbf{i}(\mathbf{l_k},\mathbf{t})) \frac{1/A_{i(l_k,t)}}{\sum_{b=1}^{J} g_b(\mathbf{i}(\mathbf{l_k},\mathbf{t}))\lambda_b^m} \quad (21)$$

where the overall sensitivity correction factors $\overline{s}_j$ are given by Eq. (17).

IV. Methods and Results

Tomograph: Data were taken on the high resolution research tomograph (HRRT). The latest HRRT scanner is a modified version of the scanner described by Ref. [8]. The new HRRT scanner has the same octagonal design, but the detector heads are different in that they instead consist of a double 10 mm layer of LSO/LYSO for a total of 119,808 detector crystals (crystal size 2.1 x 2.1 x 10 mm^3). The total number of possible LORs is 4.486x10^9.

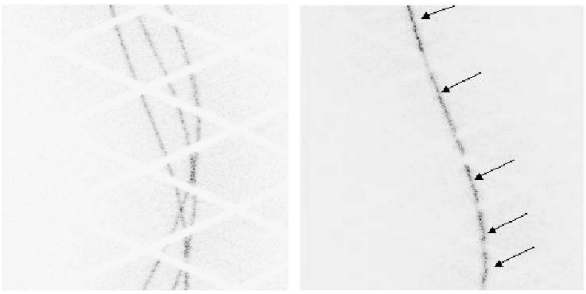

Fig. 3. Sinogram of a moving line source without (left) and with (right) motion-compensated histogramming. Direct plane #110 is shown (randomly selected). Clearly, upon appropriate histogramming, some counts are histogrammed into bins corresponding to detector gaps (shown by arrows), signifying that they would not have been detected had the object not moved.

Phantoms used and measurements performed: An F-18 line source was inserted axially into a 70-cm long NEMA phantom (20 cm diameter), placed 4cm away from and parallel to the central axis of the cylinder. The measured true count rate was 124k/s with a random fraction of 13%. Three separate frames each of duration 4 minutes were acquired with the cylinder manually rotated by ~45 degrees in-between the frames. The three frames were then combined into one single frame to study motion correction for both the histogram-mode and list-mode reconstruction schemes. Detector normalization correction factors were obtained from a 12 hour scan using a rotating rod source.

Data analysis and Results: The center of the cylinder used in the first study was expected to have undergone small translations as one rotated the object. A motion tracking system is not yet available for the scanner. In this regard, exact inter-frame rotations and translations of the phantom were measured by comparison of separate reconstructions for the three frames.

A. Histogram-mode Reconstruction: In histogram-mode, two reconstruction schemes were applied to the motion-compensated sinogram: (I) ignoring data allocated to detector gaps after motion-compensated histogramming and using the system matrix regularly used for non-moving objects. (II) the exact reconstruction algorithm proposed by Eq. (14).

Fig. (3a) shows a typical acquired sinogram, with the data from the three frames histogrammed without any motion-correction. The presence of three distinct sinogram patterns as well as the detector gaps are clearly observable. Fig. (3b) shows the resulting motion-compensated sinogram. The histogram clearly exhibits non-zero counts in certain histogram bins corresponding to detector gaps, a result of motion-compensated histogramming. Scheme I was seen to considerably underestimate the image intensity (by -18%), compared to the reference image (which did not correct for motion), whereas for the reconstruction scheme II the

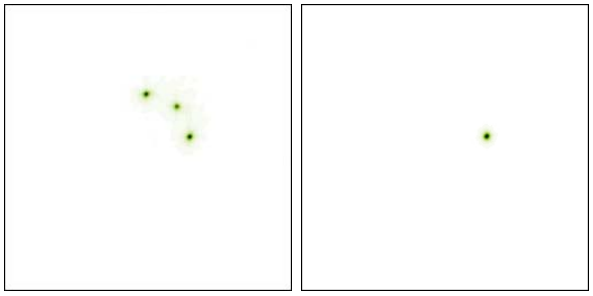

Fig. 4. Images reconstructed using list-mode algorithm a) without and b) with motion correction. Complete motion correction using rotation and translation operators results in consistent reconstruction of data. Three iteration were applied to the data. Plane 110 is shown (randomly selected).

agreement was within $\sim$1%.

B. List-mode Reconstruction: In this study, we also implemented the motion-corrected list-mode reconstruction algorithm described by Eq. (21). Ref. [11] should be consulted for details of implementation of the regular list-mode EM algorithm with random events correction on the HRRT and comparison of statistical properties with 3D-OSEM reconstruction. The data were then reconstructed: (I) without any motion correction, (II) with full (rotation+translation) motion correction, and the results were subsequently compared.

Fig. (4a) shows the image reconstructed from the overall scan without motion correction. Fully motion-corrected reconstruction (using both rotations and translations) resulted in best image quality, as depicted in Fig. (4b). The total number of counts in both images were confirmed to be within 0.5%.

V. Conclusion

This paper was intended to demonstrate and address the fact that fully motion-corrected image reconstruction cannot be performed by mere motion-compensation of the data. This fact was attributed to the existence of LORs corresponding to no actual pairs of detectors (e.g. gaps in-between detector or LORs axially out of the FOV) and their "interaction" with the detectable LORs due to motion.

It was shown that appropriate system matrix modeling of the aforementioned effects in the histogram-mode as well list-mode reconstructions ultimately modified the sensitivity correction factors. These factors, at first instance, appeared extremely time-consuming to compute for the general case of continuous motion throughout the scan. However, closer inspection revealed that use of attenuation pre-correction for the data (i.e. unweighted or N-weighted schemes) allowed computation of time-averaging of sensitivity correction factors to be performed in the image-domain, thus significantly reducing computation time required for the case of high resolution scanners in which noticeably larger number of LORs are utilized, compared to image voxels.

It was also noted that in histogram-mode reconstruction, a motion-corrected LOR does not typically correspond exactly to the center of a sinogram bin and an interpolation needs to be performed. Nevertheless, list-mode event coordinates can be maintained as continuous variables in list-mode reconstruction, therefore pointing to a potential advantage in terms of inherent accuracy in motion correction.

Acknowledgments

This work was supported by the Canadian Institute of Health Research, the TRIUMF Life Science grant, the Canada Foundation for Innovation, the Ontario Innovation Trust, the Natural Sciences and Engineering Research Council of Canada UFA (V.S.) and PGS B (A.R.) scholarships, as well as the Michael Smith Foundation for Health Research scholarship (V.S.).

References

[1] Y. Picard and C. J. Thompson, "Motion correction of PET images using multiple acquisition frames", *IEEE Trans. Med. Imag.*, vol. 16, pp. 137-144, 1997.

[2] R. R. Fulton et al, "Correction for head movement in positron emission tomography using an optical motion tracking system", in Proc. IEEE Nuc. Sci. Symp. Med. Im. Conf., vol. 17, pp. 58-62, 2000.

[3] M. E. Daube-Witherspoon, Y. C. Yan, M. V. Green, R. E. Carson, K. M. Kempner, and P. Herscovitch, " Correction for motion distortion in PET by dynamic monitoring of patient position", *J. Nucl. Med.*, vol. 31, p.816, 1990.

[4] B. J. Lopresti, A. Russo, W. F. Jones, T. Fisher, D. G. Crouch, D. E. Altenburger, D. W. Townsend, "Implementation and Performance of an Optical Motion Tracking System for High Resolution Brain PET Imaging", *IEEE Trans. Nucl. Sci.*, vol. 46, pp. 2059-2067, 1999.

[5] P. M. Bloomfield, T. J. Spinks, J. Reed, L. Schnorr, A. M. Westrip, L. Livieratos, R. Fulton, and T. Jones, "The desing and implementation of a motion correction scheme for neurological PET", *Phys. Med. Biol.*, vol. 48, pp. 959-978, 2003.

[6] J. Qi and R. H. Huesman, "Correction of Motion in PET using Event-Based Rebinning Method: Pitfall and Solution", *J. Nucl. Med.*, pp. 146P, 2002.

[7] T. J. Hebert and R. Leahy, "Fast methods for including attenuation in the EM algorithm", *IEEE Trans. Nucl. Sci.*, vol. 37, pp. 754-758, 1990.

[8] K. Wienhard, M. Shmand, M. E. Casey, K. Baker, J. Bao, L. Eriksson, W. F. Jones, C. Knoess, M. Lenox, M. Lercher, P. Luk, C. Michel, J. H. Reed, N. Richerzhagen, J. Treffert, S. Vollmar, J. W. Young, W. D. Heiss, and R. Nutt, "The ECAT HRRT: Performance and First Clinical Application of the New High Resolution Research Tomograph", *IEEE Trans. Nucl. Sci.* vol. 49, pp. 104-110, 2002.

[9] L. Parra and H. H. Barrett, "List-mode Likelihood: EM algorithm and image quality estimation demonstrated on 2-D PET", *IEEE Trans. Med. Imag.*, vol. 17, no. 2, pp. 228-235, 1998.

[10] J. Qi and R. H. Huesman, "List mode reconstruction for PET with motion compensation: a simulation study", *Proceed. of 2002 IEEE Inter. Symp. Bio. Imag. 413-416*, 2002.

[11] A. Rahmim, M. Lenox, A. J. Reader, C. Michel, Z. Burbar, T. J. Ruth, and V. Sossi, "Weighted Iterative List-Mode Reconstruction for the High Resolution Research Tomograph", VIIth International Conference on Fully 3D Reconstruction in Radiology and Nuclear Medicine, Saint-Malo, France, 2003